Journal of Power Sources 393 (2018) 161–168

Contents lists available at ScienceDirect

Journal of Power Sources

journal homepage: www.elsevier.com/locate/jpowsour

High-performance and integrated design of thermoelectric generator based on concentric filament architecture

Kai Liu[a], Xiaobin Tang[a,b,*], Yunpeng Liu[a,b], Zicheng Yuan[a], Junqin Li[a], Zhiheng Xu[a], Zhengrong Zhang[a], Wang Chen[a]

[a] Department of Nuclear Science and Engineering, Nanjing University of Aeronautics and Astronautics, Nanjing 210016, China
[b] Jiangsu Key Laboratory of Material and Technology for Energy Conversion, China

HIGHLIGHTS

- A concentric thermoelectric filament structure used for radioisotope thermoelectric generator was designed.
- The high voltage output of the thermoelectric filament was proven by comparison with that of the traditional structure.
- Thermoelectric filaments and corresponding devices were manufactured and tested.
- The designed thermoelectric generator will be a reliable power supply for space apparatus.

ARTICLE INFO

Keywords:
Brush coating
Concentric filament architecture
Finite element simulation
Radioisotope thermoelectric generator
Thermoelectric filament device

ABSTRACT

A concentric thermoelectric filament structure used for radioisotope thermoelectric generator (RTG) is designed to satisfy low-power and high-voltage demands for aerospace microelectronic devices. The thermoelectric filament is proven to have a better output voltage than the traditional thermoelectric structure by using COMSOL. The unbreakable thermoelectric filament and corresponding devices are prepared by employing a simple and easy brush coating process. A single thermoelectric filament obtains an open-circuit voltage (V_{oc}) of 6.0 mV and a maximum power output (P_{max}) of 2.0 μW at 398.15 K hot surface temperature. An array of thermoelectric filaments is fabricated for the radioisotope heat source of planar heat surface, which obtains V_{oc} of 83.5 mV and P_{max} of 32.1 μW at the hot surface temperature of 398.15 K, thereby verifying the practicability of the concentric filament structure in devices. Another radial thermoelectric filament device is designed for the cylindrical heat source. This device exports 84.5 mV V_{oc} and 42.5 μW P_{max} at the hot surface temperature of 398.15 K. These thermoelectric devices could gain larger electrical performance in small space through further series connection and fabrication, which will be a commendable design scheme for the radioisotope thermoelectric generator.

1. Introduction

A spacecraft has high requirements for life, reliability, and environmental adaptability of the power system for space exploration mission. The radioisotope thermoelectric generator (RTG), which converts decay heat into electrical energy by using a thermoelectric device, has numerous advantages, such as high reliability, long lifetime, and minimal environmental impact [1,2]. A remarkable application prospect for RTGs in the power supply of spacecraft exists [3,4]. Small-sized scientific instruments and prospecting apparatus equipped with aircrafts increase with the increase in scientific experimental missions in space exploration. Therefore, a high electrical performance requirement of miniaturized RTG for space application is presented [5].

At present, studies on RTG mainly focus on thermoelectric materials and relevant devices. Thermoelectric materials in RTGs are mostly prepared by hot pressing method. The corresponding devices usually have satisfactory thermoelectric properties by adopting the traditional π-type structure as the basic framework [6–8]. However, a few problems, such as brittle material properties and weak voltage density for low temperature difference, are observed. The open-circuit voltage (V_{oc}) of thermoelectric devices is known to be proportional to the length of the thermoelectric leg and its number in the unit area [9–11]. Richard et al. used a cutting technology to prepare slender thermocouples with a length of 0.855 in and obtained 5.1 V V_{oc} at the temperature difference of 300 K [12,13]. However, the thermoelectric leg was brittle due to the small aspect ratio, which resulted in difficulty in fabricating

* Corresponding author. Department of Nuclear Science and Engineering, Nanjing University of Aeronautics and Astronautics, Nanjing 210016, China.
E-mail address: tangxiaobin@nuaa.edu.cn (X. Tang).

https://doi.org/10.1016/j.jpowsour.2018.05.018
Received 13 December 2017; Received in revised form 24 February 2018; Accepted 5 May 2018
0378-7753/ © 2018 Elsevier B.V. All rights reserved.

Nomenclature

A	Cross-sectional area of thermoelectric leg
L	Length of a thermoelectric leg, mm
P_{max}	Maximum output power of the RTG, W
P_{out}	Output power of the RTG, W
P_{th}	Input power of the heat source surface per unit area, W m^{-2}
R	External load resistance in the RTG, Ω
R_{th}	Thermal resistance of the P/N thermoelectric leg, K W^{-1}
V	Output voltage of the RTG, V
V_{oc}	Open-circuit voltage of the RTG, V
n	Number of thermoelectric legs
r	Internal resistance in the RTG, Ω
r_1	Radius of the internal N-type thermoelectric material, mm
r_2	Radius of the middle insulating material, mm
r_3	Radius of the external P-type thermoelectric material, mm
ΔT	Temperature difference of the hot and cold sides of RTG
Σ	Electrical conductivity, S m^{-1}
α	Seebeck coefficient, V K^{-1}
κ	Thermal conductivity, W m^{-1}·K^{-1}

thermoelectric devices. A few researchers currently utilize high precision equipment to prepare tens of thousands of micro thermoelectric legs in a unit area to achieve high-voltage output [14–16]. Xie et al. prepared the micro thermoelectric device by using chemical vapor deposition. The V_{oc} was 16.7 V in 1 cm^2 under the 5 K temperature difference, but the output power was low [17]. In general, microelectronics-based thermoelectric devices are unsuitable for large temperature difference and show poor practicality for inevitably large resistance.

Therefore, aiming at the demand of aerospace microelectronic devices for low power consumption and high voltage, this paper originally designed a concentric thermoelectric device with better voltage output, which is proven to be superior to the traditional structure by the finite element simulation. The unbreakable thermoelectric filaments were prepared by simple painting, and the electrical output performance was obtained. For different heat transfer modes of miniature radioisotope heat source, two functional devices, including arrayed and radial thermoelectric filament devices, were designed. Through further series connection and fabrication, the thermoelectric array could gain greater output voltage and power in smaller space. It can deal with the voltage and power requirements of different space components. These devices provide a feasible scheme for the power supply of space apparatus.

2. Structural design and simulation analysis

2.1. Concentric filament structure

Fig. 1 shows the structure of concentric thermoelectric filament, which comprises P/N thermoelectric and insulating materials. The thermoelectric filament is similar to combinatorial concentric circles. The P/N thermoelectric materials are insulated by the insulating material. The current initially flows through the inner N-ring into the outer P-ring and then flows out. The edge of the outer P-type ring is connected with the end point of N-type in another filament through the copper wire. The traditional π-type thermoelectric structure comprises separate P/N thermoelectric legs, as shown in Fig. 2(b). Compared with the π-type structure, the concentric filament architecture takes the separated P/N thermoelectric legs into a concentric whole. This architecture effectively realizes the reasonable utilization of the inner space from the thermoelectric device. Moreover, this structure can obtain a small aspect ratio, thereby resulting in relatively large temperature differences and improved electrical properties. The equations of the open-circuit voltage and the output power (P_{out}) of the thermoelectric filament device under steady state are obtained by analyzing the structure of the thermoelectric filament as follows:

$$V_{oc} = \alpha \times \nabla T \cdot n, \tag{1}$$

$$P_{out} = \frac{V^2}{(R + r)^2} \cdot R, \tag{2}$$

where V_{oc}, which is the maximum value of the output voltage, is the product of Seebeck coefficient (α), temperature difference (ΔT), and the number of thermoelectric legs. P_{out} changes with the external load resistance (R) and the internal resistance (r) of the RTG. The definition of thermal resistance (R_{th}) and the relationship between R_{th} and thermal conductivity (κ) can be expressed as follows:

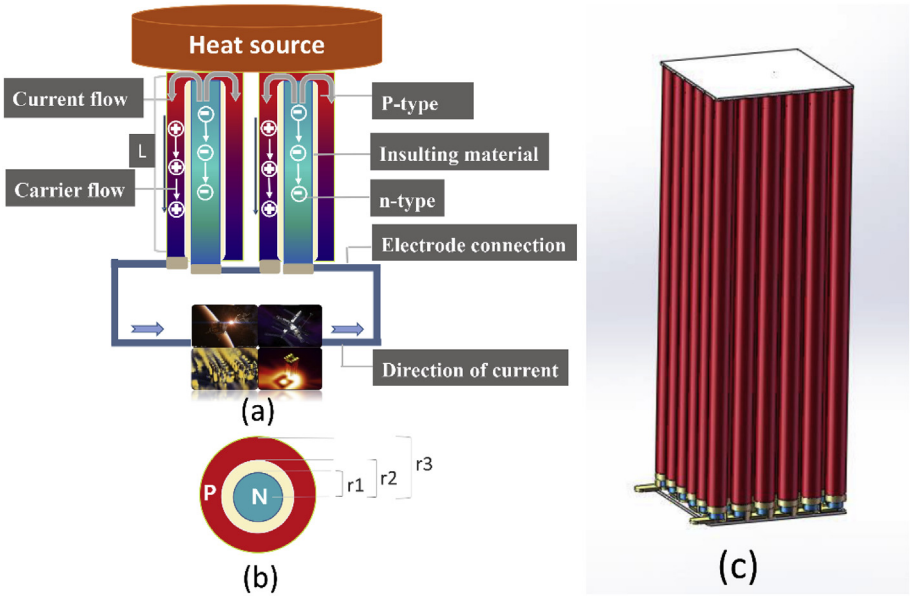

Fig. 1. (a) Pair of thermoelectric filaments based on concentric thermoelectric filament architecture; (b) Sectional view; (c) Arrayed thermoelectric devices in series.

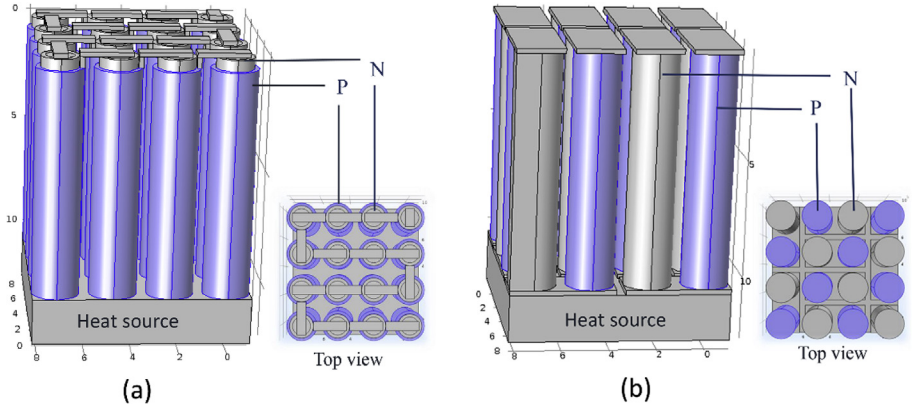

Fig. 2. Two types of structural diagrams (a) concentric filament structure; (b) traditional π-type structure.

$$R_{th} = \frac{\Delta T}{P_{th}} = \frac{\mathrm{L}}{\kappa \cdot \mathrm{A}}, \tag{3}$$

where P_{th} is the input power of the heat source surface, L is the length of a thermoelectric leg, and A is the cross-sectional area of thermoelectric leg. The ultimate V_{oc} and P_{out} were obtained by substituting R_{th} into Eqs. (1) and (2), respectively:

$$V_{oc} = \alpha \times \frac{\mathrm{L} \cdot P_{th}}{\kappa \cdot \mathrm{A}} \cdot n, \tag{4}$$

$$P_{out} = \left(\alpha \times \frac{\mathrm{L} \cdot P_{th}}{\kappa \cdot \mathrm{A}} \cdot n\right)^2 \cdot \frac{R}{(R + r)^2}. \tag{5}$$

When the thermoelectric material and P_{th} are determined, V_{oc} of the thermoelectric device is proportional to L and n of the thermoelectric leg and inversely proportional to κ and A, as shown in Eq. (4). P_{out} is a variable quantity of V_{oc} and r, and P_{max} is obtained in Eq. (2) when $R = r$.

2.2. Simulation verification

COMSOL software was used to simulate its thermoelectric conversion process to verify the feasibility of the thermoelectric filament architecture in principle. First, the geometric model of the thermoelectric filament device was established, as shown in Fig. 2(a). The traditional π-type thermoelectric structure in Fig. 2(b) was also constructed for comparison. The related structural parameters are shown in Table 1. A cuboid shell wrapped these thermoelectric devices, and thermal insulating materials filled the inner gaps. The bottom cuboid was a simulated radioisotope heat source. Notably, the cross-section area ratios of P-type to N-type thermoelectric materials in both structures are 1:1. The volume of all P/N materials in the thermoelectric filament structure is only 72% of that in the traditional structure due to the addition of the insulating material inside the filament. Properties of materials used in COMSOL is seen in Table 2.

The surface temperature of the simulated heat source ranged from 323.15 K to 398.15 K according to the measured temperature of the radioisotope heat source used in mini-RTGs in this section [18,19]. This setup determined the hot surface and uncertain cold surface temperatures to simulate the real RTG process. The electrical performance of the thermoelectric device was obtained at different temperatures. Fig. 3(a) shows the temperature field distribution of the thermoelectric filament device under a surface temperature of 398.15 K. The temperature difference between the two ends of the thermoelectric device reaches 78.9 K. Fig. 3(b) shows the potential field distribution of the device. The electric potential increases from the upper-right corner to the lower-right corner from the top view. What's more, it first increases from top to bottom in the inner ring, and then increases from bottom to top in the outer ring. Fig. 3(c) and (d) show that the thermoelectric filaments connected in series obtained 535.6 mV and 19.8 mW V_{oc} and P_{max}, respectively. The internal resistance of the device is 3.62 Ω, which is calculated by the simulation method.

When the hot surface temperature of the simulated heat source changes from 323.15 K to 398.15 K, the output power of the thermoelectric filament device is nearly similar to that of the traditional structure device, as shown in Fig. 3(d). However, the V_{oc} of the former device is always approximately 2.4 times higher than that of the latter device at the same temperature condition, as shown in Fig. 3(c). This phenomenon can be attributed to the changing values of A, n, and κ in Eq. (3). The A of P/N thermoelectric material in thermoelectric filaments was less than half of the traditional structure; hence, the n of the former becomes twice than that of the latter, thereby resulting in a positive V_{oc} growth of the thermoelectric filament. In addition, the adjunction of the insulation material decreased κ for the thermoelectric filament, which indirectly increased R_{th}. Therefore, the ΔT between the two ends of filaments increases. The overall voltage of the device is 2.4 times the traditional structure because the volume of thermoelectric materials in the thermoelectric filament reduced 28% less than the traditional structure. The r increases with the increasing number of P/N junction in the thermoelectric filament, and the difference between the output powers of the two structures finally becomes small. Thus, the concentric thermoelectric filament can output high voltage in the proposition of ensuring normal electrical power output, which is in agreement with the demand of high voltage and low power consumption for small space electronic apparatus.

3. Experimental preparation and performance testing

3.1. Single thermoelectric filament

In the experimental preparation, the constantan wire (r_1 = 0.75 mm) was taken as an N-type thermoelectric material and was cut to 30 mm long. This metal wire has excellent toughness and is currently one of the best N-type metal thermoelectric materials [20]. The resin-based insulation coating was selected because the insulating material in the intermediate layers benefits from its amenable brushing and forming. This insulation coating can resist high temperature of up

Table 1
Parameters of two simulated structures.

Structures	Internal diameter r_1/mm	Middle diameter r_2/mm	Outer diameter r_3/mm	Height L/mm	P/N cross-section area ratio
Concentric filament	0.6	0.8	1	10	1:1
Traditional π-type	–	–	1	10	1:1

Table 2
Properties of materials used in COMSOL.

Type	P/N-type	Insulating material
Density(g cm^{-3})	7.7	0.2
Atmospheric heat capacity C_p (J Kg^{-1} K^{-1})	154	10–24
Electrical conductivity σ (10^5 S m^{-1})	0.59–1.43	_
Seebeck coefficient α (μV K^{-1})	± (168–237)	_
Thermal conductivity κ (W m^{-1} $K^{-2)}$)	1.6–2.4	0.02

300 °C. The P-type thermoelectric material adopted was a self-configuring thermoelectric paint. The P-type Bi_2Te_3 powder was mixed with DER732 Binder (polypropylene glycol delicious epoxy resin) at a mass ratio of 88:10, thereby following a well-proportioned agitation. Fig. 4 shows that the insulating layer was first coated on the surface of the constantan wire. The layer thickness was mostly 0.13 mm–0.18 mm. After high-temperature drying, the insulating layer on the metal wire at two terminals was removed. Second, the P-type thermoelectric paint was coated on the surface of the insulating layer and one end of the metal wire, and then was dried. The other end of the metal wire was not coated. Its position is far away from the hot surface of heat source. After sintering at 573.15 K for 5 h, the thermoelectric filament was prepared. Third, the edge of the outer P-type ring was connected with wires. Subsequently, the conductive silver paste was coated at the contact point to stabilize the connection and reduce contact resistance. Finally, the filament was tentatively prepared.

The electrical performances of thermoelectric filaments were tested using the parameter analyzer (Keithley 4200 SCS) at an ambient temperature of 293.15 K. An electric heating platform or an electric heating rod was considered a radioisotope heat source to provide constant temperature (323.15 K–398.15 K), as shown in Fig. 5. The testing of the samples was performed after being placed on the platform for half an hour to minimize the error and improve the accuracy of the measurement data. The internal temperature of the filament stabilized at that time. The real-time temperatures of the hot and cold sides of the thermoelectric filament were measured by the temperature sensor (R7100).

After repeated experiments and preparation, thermoelectric filaments were proven to have stable performance and good reproducibility. One of the thermoelectric filaments was selected. The radius of this filament is 1.27 mm, and its internal resistance is 3.1 Ω at room temperature. Under the control of the electric heating platform, the *I–V* curves of the thermoelectric filament were measured at the hot end temperature of 323.15 K–398.15 K, as shown in Fig. 6. The electrical properties of the N-type constantan wire used in the preparation were also tested. The *I–V* curves of the single thermoelectric filament and constantan wire were approximately a straight line. The voltage and output power increased with the increase in heating temperature. The V_{oc} of 6.0 mV and P_{max} of 2.0 μW were obtained at the hot surface temperature of 398.15 K (at this time, the temperature difference is 61.2 K). In comparison, the constantan wire only has 0.55 mV V_{oc} and 0.02 μW P_{max}. Fig. 6(c) reflects the relationship between the V_{oc} and P_{max} of the thermoelectric filament and the hot end temperature. The temperature difference increases with the increase in hot end

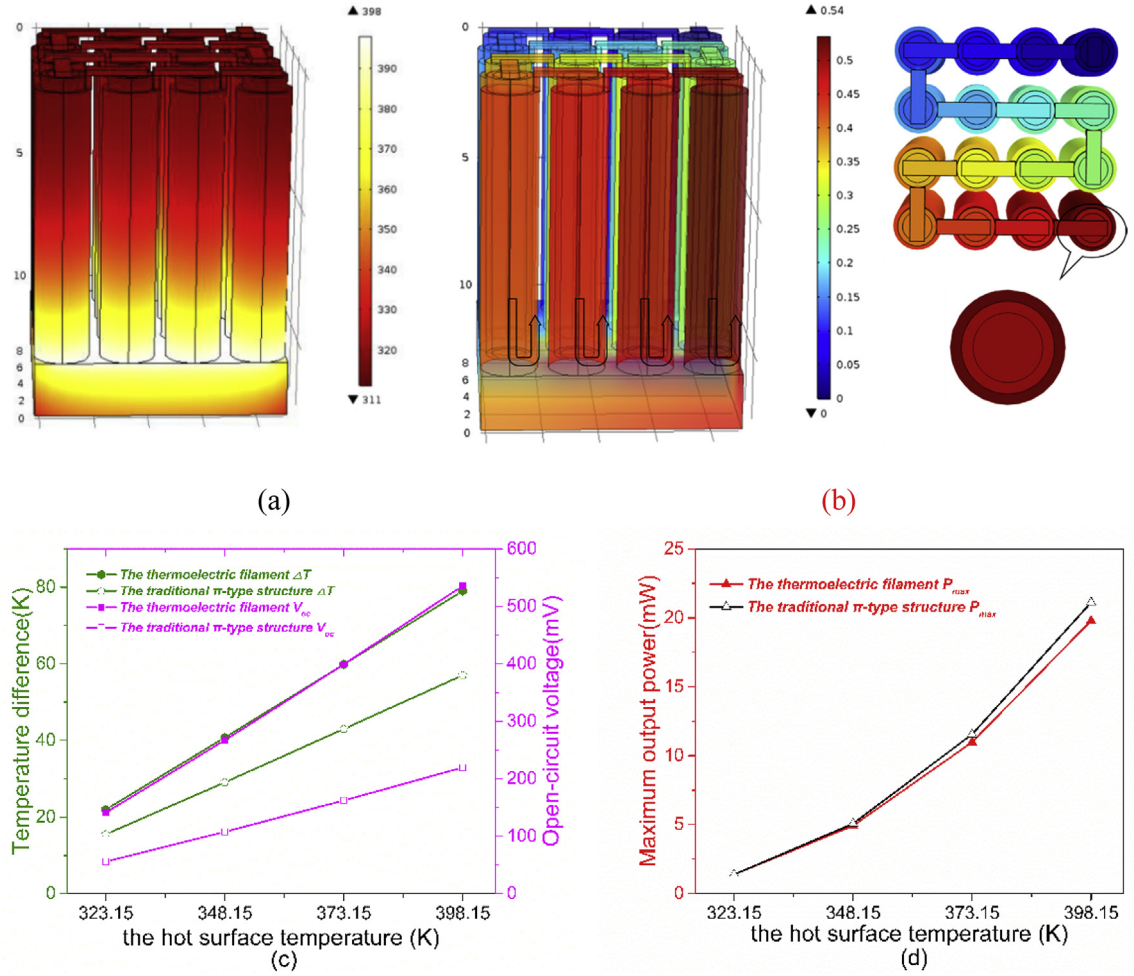

Fig. 3. (a) Temperature field distribution and (b) potential field distribution at 398.15 K hot surface temperature of the thermoelectric filament device; (c) ΔT, V_{oc} and (d) P_{max} of thermoelectric filament device and traditional π-type device vs hot surface temperature.

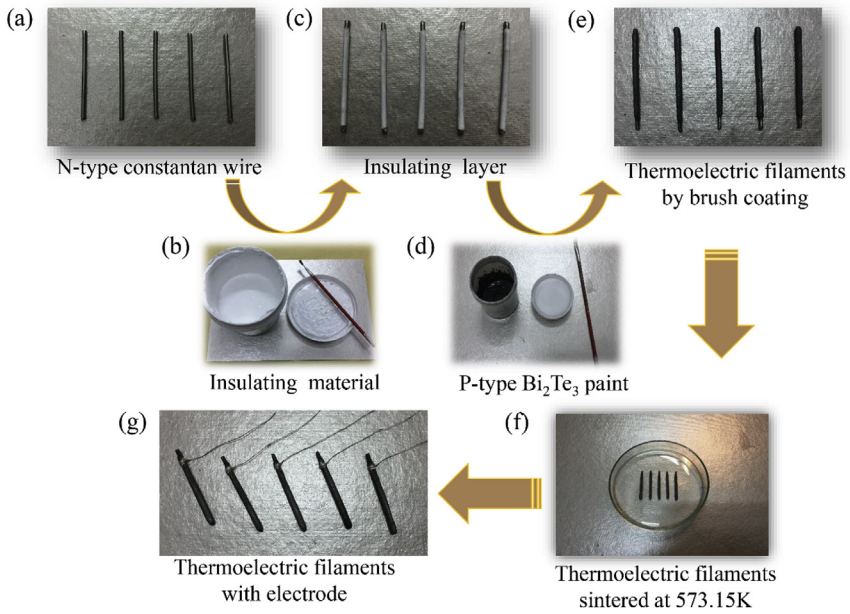

Fig. 4. Preparation of concentric thermoelectric filament. (a–c) preparation of insulating layer; (d–e) preparation of P-type Bi_2Te_3 paint; (f) prepared thermoelectric filament by sintering; (g) thermoelectric filament with electrode.

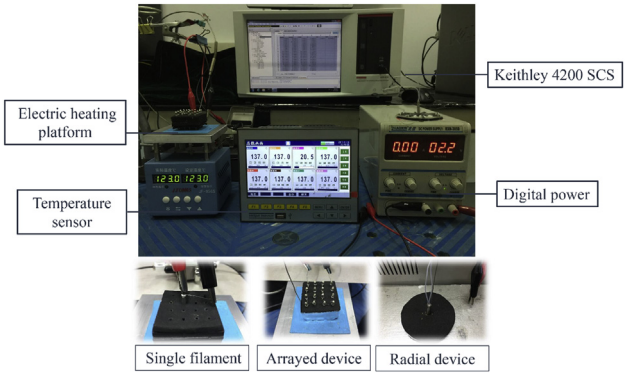

Fig. 5. Electrical test chart of the thermoelectric filament devices.

temperature. V_{oc} and P_{max} show a linear increase with the increase in hot end temperature, which is consistent with the thermoelectric properties of thermoelectric materials. This result indicates the feasibility of the concentric filament structure. Fig. 6(d) reflects the relationship between V_{oc} and P_{max} of the constantan wire and the hot end temperature. Compared with the metal wire, the concentric circle structure and simple preparation considerably improved the thermoelectric properties of thermoelectric filaments, thereby providing a new preparation approach for the thermoelectric unit.

3.2. Arrayed thermoelectric filament device

An arrayed thermoelectric filament device was fabricated considering that the heat surface of radioisotope heat source is possibly planar, as shown in Fig. 7(a). Initially, 16 thermoelectric filaments were combined into a 4 × 4 three-dimensional array. The thermal insulation foam was filled in this array. The edge of the outer P-type ring in one filament was connected with the end point of the N-type wire in another filament by conductive wire. Subsequently, the conductive silver paste was coated at the contact point. Finally, the arrayed thermoelectric device was completed.

The fabricated arrayed thermoelectric device has a dimension of 40 × 40 × 30 mm^3. This device has an internal resistance of 53.5 Ω at room temperature. As shown in Fig. 5, the *I–V* curves of the thermoelectric device were tested at the hot surface temperature of 323.15 K to 398.15 K by controlling the electric heating platform. In Fig. 7 (b), the voltage of the array thermoelectric device linearly decreases with the increase in the current. The voltage and the power output increase with the increase in hot end temperature. The 83.5 mV V_{oc} and 32.1 μW P_{max} were obtained at the hot end temperature of 398.15 K (at this time, the temperature difference reaches 65.6 K). Fig. 7(c) reflects the relationship between V_{oc} and P_{max} of the thermoelectric device and the hot surface temperature. The temperature difference between hot and cold ends increases with the increase in hot end temperature. V_{oc} and P_{max} increase with the increase in hot end temperature in an approximately linear relationship. The test results show that the thermoelectric filament can be successfully fabricated to a thermoelectric device. This thermoelectric device can be well applied to RTGs by combining with the radioisotope source. Through further series connection and fabrication, the thermoelectric array could obtain large output voltage and power in a small space, which is expected to provide practical power for space components.

3.3. Radial thermoelectric filament device

The structural design of a radial thermoelectric filament device was proposed considering that the radioisotope heat source is cylindrical in most cases. First, the one-side ends of eight thermoelectric filaments near the heat source were coated with a layer of sealant. Second, eight thermoelectric filaments were arranged in a radial structure on an insulating substrate. The uncoated ends of filaments on the other side were sticking straight out of the circle. Third, the thermoelectric filaments were connected with conductive wires and silver paste. Finally, a single-layer radial thermoelectric filament device with eight filaments was achieved, as shown in Fig. 8(a). The measured internal resistance at room temperature is 32.9 Ω, and its outer diameter is 30 mm. The ceramic electric heating rod was placed in the middle of the device as an equivalent heat source [21–23]. The electrical properties of radial thermoelectric filament device were tested while continuously providing stable heat, as shown in Fig. 5. The surface temperature of the electric heating rod remained in the range of 323.15 K–398.15 K by controlling the input current and voltage of electric heating rod.

Fig. 8(b) shows the *I–V* curves of radial thermoelectric filament device of a single layer as a temperature function. Fig. 8(c) reflects the

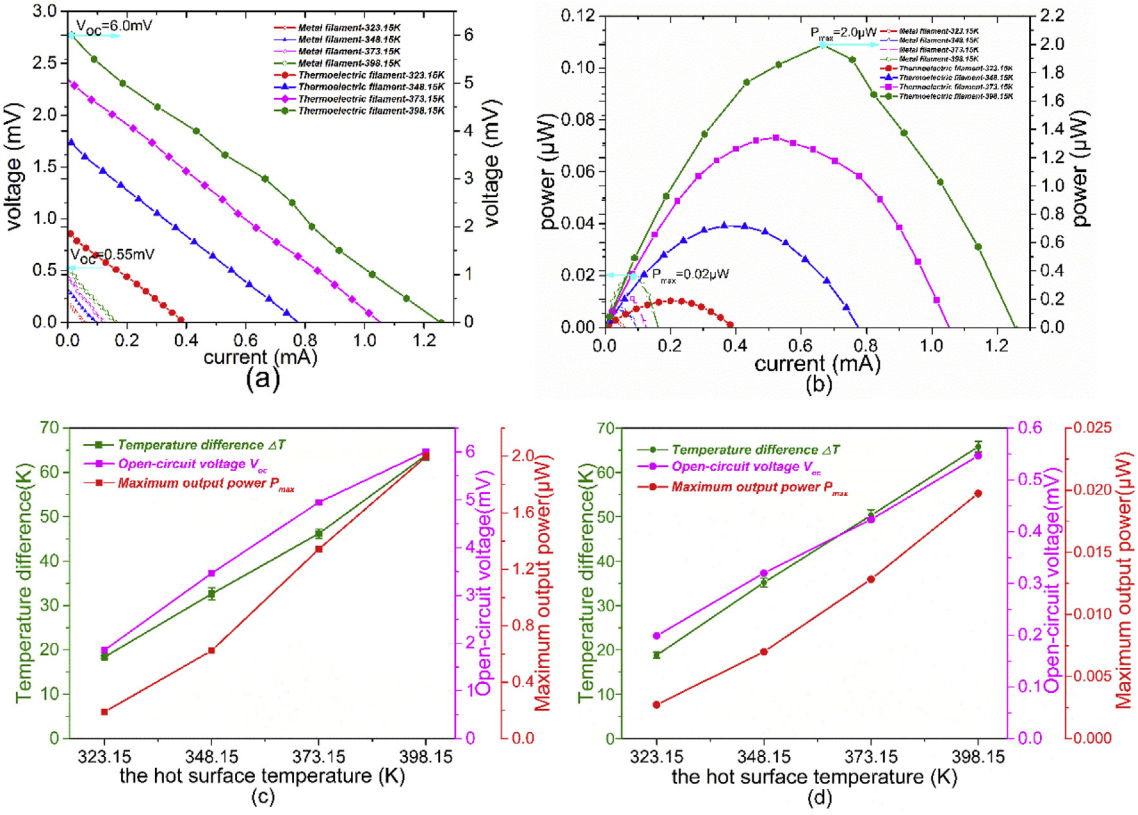

Fig. 6. (a) $I - V$ characteristic curves; (b) $I - P$ characteristic curves; (c) ΔT, V_{oc}, and P_{max} of single thermoelectric filament vs. hot surface temperature; (d) ΔT, V_{oc}, and P_{max} curve of single constantan wire vs. hot surface temperature.

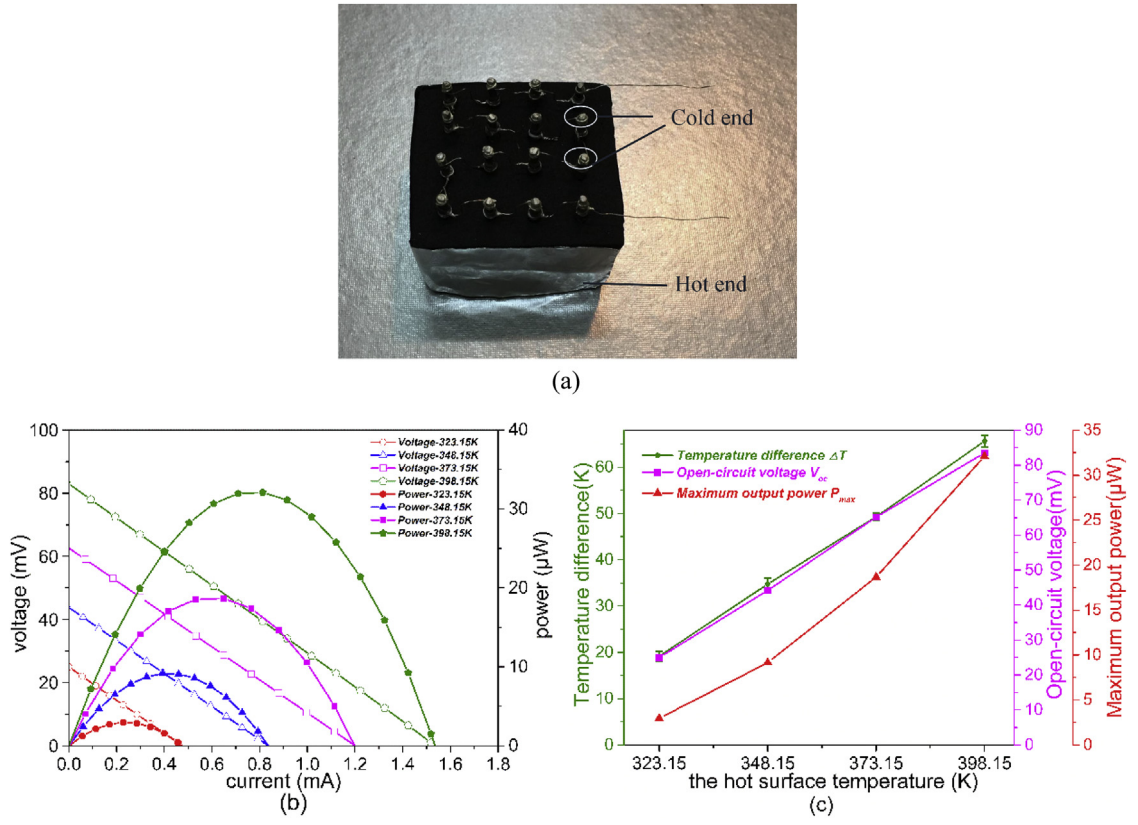

Fig. 7. (a) Arrayed thermoelectric filament device; (b) $I - V$ characteristic curves; (c) ΔT, V_{oc}, and P_{max} vs. hot surface temperature.

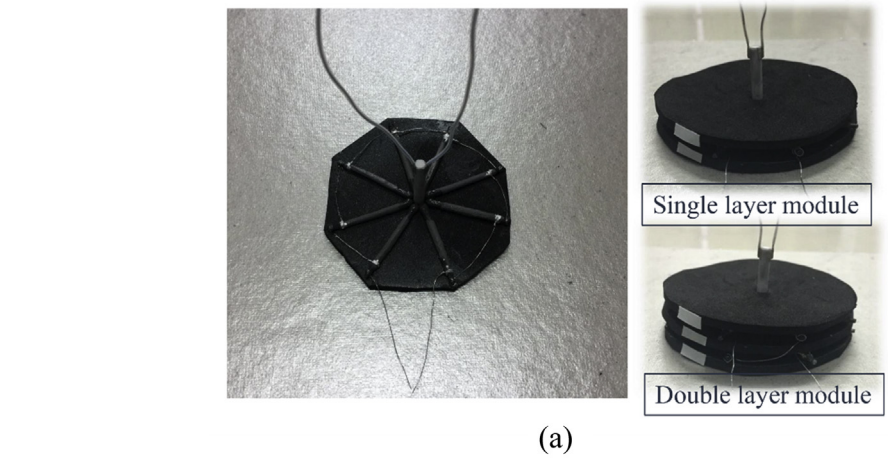

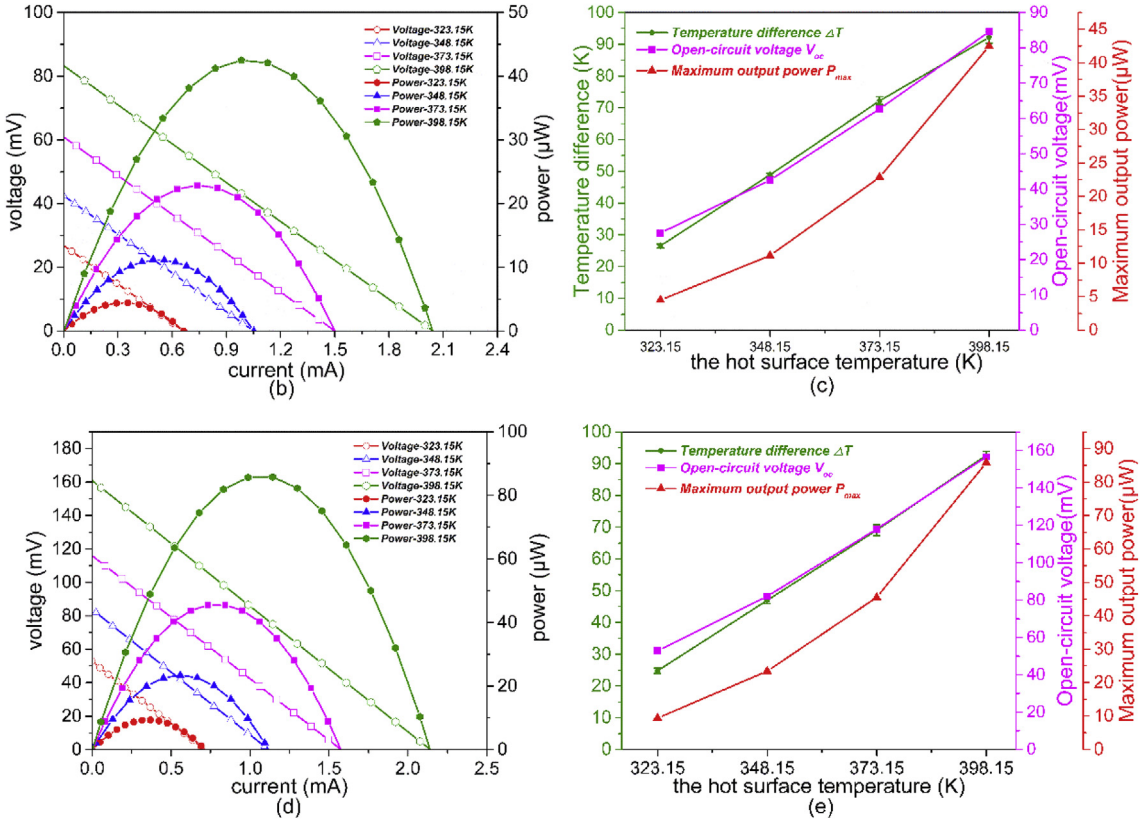

Fig. 8. (a) Radial thermoelectric filament device with single or double layers; (b–c) Electrical properties of a single radial thermoelectric filament device; (d–e) Electrical properties of a double radial thermoelectric filament device.

relationship between V_{oc} and P_{max} of the single radial thermoelectric device and the hot surface temperature. When the hot surface temperature is 398.15 K, the temperature difference reaches 92.1 K. The output values of V_{oc} and P_{max} reached 84.5 mV and 42.5 μW, respectively. In addition, the stacked design could combine additional radial devices together to achieve a large voltage output. Thus, a double-layer radial thermoelectric filament device was manufactured, as shown in Fig. 8(a). The corresponding result is shown in Fig. 8 (d) and (e). When the hot surface temperature is 398.15 K, the V_{oc} and P_{max} is 156.7 mV and 85.8 μW, respectively. The double-layer radial thermoelectric filament device obtained approximately twice as that of the voltage and power of the single-layer structure. Therefore, RTGs will obtain a large electrical output by stacking additional multi-layer devices. The radial structure resulted in a larger temperature difference at the same hot surface temperature than the previous arrayed structure. Thus, the radial thermoelectric filament device achieved an ideal electrical output with few thermoelectric filaments. The preceding results mentioned indicate that the radial thermoelectric filament device is a feasible component for RTGs and provides good reference significance for the next generation of thermoelectric devices.

4. Conclusion and prospect

A high-voltage thermoelectric generator is proposed in this paper based on the concentric filament architecture. The COMSOL simulation results show that V_{oc} of thermoelectric filament device is approximately 2.4 times that of the traditional π-type structure device. The concentric filament structure is proven to have high-voltage output through the reasonable analysis of corresponding equations. The thermoelectric filament is prepared by simple brush coating. The V_{oc} of 6.0 mV and the

P_{max} of 2 μW are obtained under the hot terminal temperature of 398.15 K. An arrayed thermoelectric filament device with 4 × 4 filaments is fabricated for the radioisotope heat source of planar heat surface. When the hot surface temperature is 398.15 K, the V_{oc} is 83.5 mV and the corresponding P_{max} is up to 32.1 μW. In addition, another radial thermoelectric filament device is prepared to facilitate the suitability of the RTG to the cylindrical heat source. The radial thermoelectric filament device of a single layer with eight filaments achieves V_{oc} of 84.5 mV and P_{max} of 42.5 μW and that of double layer with 16 filaments achieves V_{oc} of 156.7 mV and P_{max} of 85.8 μW at a hot surface temperature of 398.15 K. The arrayed and radial thermoelectric filament devices based on concentric filaments have been proven to show a considerable potential in the application of the radioisotope thermoelectric generator. A greater electrical performance will be obtained by further integrated combination. This paper provides a good structural design as a trial and verification. It could satisfy the low-power and high-voltage demand for aerospace microelectronic devices. For the next step, we will focus on optimizing device size and updating manufacture process, which aim to significantly promote the performance of this kind of thermoelectric device.

Acknowledgements

This work was supported by the National Natural Science Foundation of China (Grant No. 11675076), the National Natural Science Foundation of China (Grant No. 11505096), the Natural Science Foundation of Jiangsu Province (Grant No. BK20150735), the Jiangsu Planned Projects for Postdoctoral Research Funds (Grant No. 1601139B), the Shanghai Aerospace Science and Technology Innovation Project (Grant No. SAST2016112).

References

[1] R.G. Lange, W.P. Carroll, Review of recent advances of radioisotope power systems, Energy Convers. Manag. 49 (2008) 393–401.
[2] J.A. Hamley, Radioisotope Power Systems Program: a Program Overview, (2016).
[3] L. Summerer, K. Stephenson, Nuclear power sources: a key enabling technology for planetary exploration, Proc. IME G J. Aero. Eng. 225 (2011) 129–143.
[4] G.R. Schmidt, T.J. Sutliff, L.A. Dudzinski, Radioisotope Power: a Key Technology for Deep Space Exploration, InTech, 2008.
[5] C.R. Chatwin, Satellite & Space Systems - Electrical Power Systems, (2017).
[6] J. Yu, H. Zhao, A numerical model for thermoelectric generator with the parallel-plate heat exchanger, J. Power Sources 172 (2007) 428–434.
[7] F. Wu, W. Wang, X. Hu, M. Tang, Thermoelectric properties of I-doped n-type Bi_2Te_3-based material prepared by hydrothermal and subsequent hot pressing, Prog. Nat. Sci. Mater. Int. 27 (2017).
[8] T. Zhang, J.M. Chen, J. Jiang, Y.L. Li, W. Li, G.J. Xu, Thermoelectric properties of the Bi_2Te_3 compound prepared by an aqueous chemical method followed by hot pressing, J. Electron. Mater. 40 (2011) 1107–1110.
[9] B. Jang, S. Han, J.Y. Kim, Optimal design for micro-thermoelectric generators using finite element analysis, Microelectron. Eng. 88 (2011) 775–778.
[10] K. Liu, Y. Liu, Z. Xu, Z. Zhang, Z. Yuan, X. Guo, Z. Jin, X. Tang, Experimental prototype and simulation optimization of micro-radial milliwatt-power radio-isotope thermoelectric generator, Appl. Therm. Eng. 125 (2017).
[11] Z. Yuan, X. Tang, Y. Liu, Z. Xu, K. Liu, Z. Zhang, W. Chen, J. Li, A stacked and miniaturized radioisotope thermoelectric generator by screen printing, Sensor. Actuator. 267 (2017).
[12] R.W. Drinker, A. Reddy, B. Heshmatpour, G.J. Snyder, K.L. Tuttle, Advanced superlattice BiTe-PbTe/TAGS milliwatt radioisotope power system, Space Technology & Applications Intforum-sta, 2005, pp. 410–420.
[13] L.A. Flanders, R.W. Drinker, B. Heshmatpour, D.S. Moul, J.P. Fleurial, K.L. Tuttle, Improvements in materials and processes for segmented BiTe/PbTe-BiTe/TAGS/PbSnTe based thermoelectric generators, Space Technology & Applications International Forum-staif, 2005, pp. 564–571.
[14] L. Janak, Z. Ancik, J. Vetiska, Z. Hadas, Thermoelectric generator based on MEMS module as an electric power backup in aerospace applications, Mater. Today Proc. 2 (2015) 865–870.
[15] Z.H.A. Rahman, M.H.M. Khir, Z.A. Burhanudin, A.A.A. Rahman, W.A.W. Jamil, Design of CMOS-MEMS based thermoelectric generator, Micro Nanoelectron. IEEE (2014) 9–12.
[16] W. Wang, Xialiao, Y. Zhu, H. Xu, H. Li, A high packing density micro-thermoelectric power generator fabricated by electrochemical MEMS technology, Procedia Eng. (2011) 85–93.
[17] J. Xie, C. Lee, H. Feng, Design, fabrication, and characterization of CMOS MEMS-based thermoelectric power generators, J. Microelectromech. Syst. 19 (2010) 317–324.
[18] V.V. Gusev, A.A. Pustovalov, N.N. Rybkin, L.I. Anatychuk, B.N. Demchuk, I.Y. Ludchak, Milliwatt-power radioisotope thermoelectric generator (RTG) based on Plutonium-238, J. Electron. Mater. 40 (2011) 807–811.
[19] A. Pustovalov, Mini-rtgs on Plutonium-238: Development and Application, (1999), pp. 509–520.
[20] R.E. Bentley, Handbook of Temperature Measurement, Springer, 1998.
[21] T.F. Hursen, S.A. Kolenik, Nuclear energy sources, Ann. N. Y. Acad. Sci. 167 (1969) 661.
[22] A. Pustovalov, V. Gusev, A. Borshchevsky, A. Chmielewski, Experimental confirmation of milliwatt power source concept, Eighteenth International Conference on Thermoelectrics, 1999, pp. 500–504.
[23] S.A. Whalen, C.A. Apblett, T.L. Aselage, Improving power density and efficiency of miniature radioisotopic thermoelectric generators, J. Power Sources 180 (2008) 657–663.